Investigation of Different Plasma Components Confinement and Turbulence Characteristics in T-10 Tokamak

V.A. Vershkov 1), D.A. Shelukhin 1), S.V. Krylov 1), A.Yu. Novikov 1), Yu.D. Pavlov 1), A.V. Khmara 1), A.N. Obysov 1), A.O. Urazbaev 1), V.M. Timokhin 2), V.A. Skokov 2)

1) NFI RRC "Kurchatov Institute", Moscow, RF
2) St.-Petersburg State Polytechnic University, St.-Petersburg, RF

e-mail address of main author: vershkov@nfi.kiae.ru

Abstract. The turbulence plasma state was characterized by means the comparison of impurity and energy confinement times. The transport of high *Z* ions was studied using KCl and Ti pellet injection and fast argon gas puffing. The impurities transport was analyzed by means of X-ray crystal monochromator RM-2. Main plasma confinement was investigated, using D_2 gas puff and energy time was estimated from the total heating power and total energy in plasma. In the neoclassical case, the different plasma species should have different confinement times, in contrast to the conditions of strong convective cells turbulence, where the transport could be the same for all plasma components. The confinement times were equal in Ohmic plasma and have similar density dependence. They greatly decreased with increase of ECRH power in agreement with L-mode energy confinement ITER scaling and became slightly different in ECRH discharges, suggesting additional deterioration of the electron energy transport due to possible appearance of electron Larmour scale turbulence in ECRH in addition to the long-wave drift one, which is dominant in the OH discharges. The decrease of the confinement with heating power is in good correlation with the increase of the turbulence level. The reflectometry experiments with the newly installed HMFS antenna, using low frequency extraordinary wave, showed that the turbulence level at HMFS lower in a factor of two, with respect to the LMFS one. This level at HMFS does not increase in ECR heated plasmas, suggesting the ballooning turbulence nature. The relative contrast of the quasi-coherent maxima in the spectrum at HMFS was much less then at LMFS.

1. Introduction.

The turbulence investigations in tokamaks have the final goal to understand and control the anomalous plasma transport. The study of the characteristics of the fluctuations of the ion Larmour scale was one of the main topics of the T-10 program for the last decade and the summary of these works was published in [1]. The new results, presented in this paper, enable deeper insight in the turbulence structure by means of characterization of the poloidal asymmetry of the different turbulence types. They were obtained with the recently installed reflectometry antenna array in the equatorial plane at the High Magnetic Field Side (HMFS) of the T-10. The confinement of the impurities and the main ions have been studied in T-4 in 70th [2,3,4]. The experiments with impurities confinement were continued in T-10 [5,6] with the addition of the studies of the electron density diffusion with single and periodic gas modulation technique [5,7]. Previous experiments were carried out in the Ohmic plasma, and neither comparison of the confinement of different plasma species with each other and no correlation with the turbulence characteristics were done. In given paper the confinement and turbulence experiments were done in parallel in OH and ECRH discharges of T-10 tokamak.

2. Energy and particle confinement.

The confinement of the plasma electron density, highly charged impurities and energy were compared at different plasma densities in OH and ECRH regimes. It should be specially stressed that such comparison will be meaningful only if all compared confinement times will characterized the transport of the core plasma in the gradient zone and the perturbation, introduced by the investigation technique, should be minimized in order that the results may characterized the properties of the unperturbed discharges. The energy confinement was

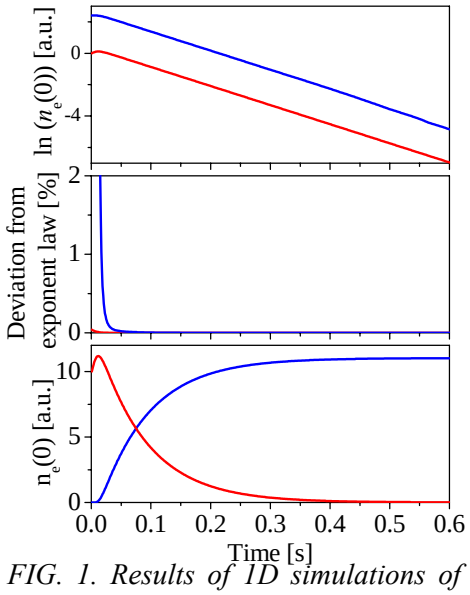

FIG. 1. Results of 1D simulations of non-recycling (red) and 100% recycling (blue) impurity behavior. Simulation parameters was a = 0.3 m, $V_p(r)$ [$m \cdot s^{-1}$] = 8·r/a; D = 0.5 $m^2 \cdot s^{-1}$.

directly calculated as $\tau_E = W_{pl}/P_{in}$, where W_{pl} was total stored plasma energy and P_{in} was the total heating power. The radiation and charge exchange losses were located mainly at the periphery, so they were not taken into account. The estimated core radiation losses inside 2/3 plasma radius lead to corrections in OH discharges less then 10% and in ECRH less then 5 %, which is comparable with the accuracy of experiment. As in OH and ECRH the heated power was input in the electron component in the central regions, so τ_E mainly characterized the electron heat conduction in the core plasma. Also, by the definition, it is related to the steady state conditions. The high *Z* impurities and electron density core confinements were determined in accordance with the known expression for τ^* as $\tau^* = \tau_p/(1-R)$, where τ_p – is the core particle confinement, *R* – is recycling coefficient and τ^* is the experimentally observed particle decay time. For the case of the injection of K and Ti recycling *R* was practically zero and their experimental decay times τ^* practically coincide with τ_p. In difference to K and Ti recycling *R* for Ar and electron density was practically near 100%. It means that their central concentration approach the steady state level after injection in accordance with the expression $N(0,t)=(1–\exp(-t/\tau_p))$. So for such cases the core particles confinement times τ_p were determined from the rate of approaching of the steady state level in the plasma center. The central Ar and electron density concentration was obtained using Abel inversion of chord X-ray and interferometer measurements. The experimental values, obtained with such technique from non-recycling K, Ti and 100% recycling Ar impurities were in good agreement, as was expected. Figure 1 just presents the results of 1D simulations of the time behavior of the central density after short injection for the case of non-recycling and 100% recycling species. The simulations were done with the same values of diffusion coefficient *D* and pinch velocity V_p. It is clear seen that the time behavior is different (Fig.1c), while the slopes of the logarithms of the densities just the same (Fig.1a). Thus the confinement times from the decay times of the non-recycling component will be equal to the one, determined from the rates of the approaching the steady state for 100% recycling. These confinement times will characterize the core plasma for both cases. It should be noted that experimental confinements were calculated after some time delay from the injection, when the plasma perturbations became small. So the confinement of the non-recycling K and Ti were obtained from the exponential time decay after injection. In case of 100% recycling Ar and electron density the confinement times were obtained from the exponential approach to the steady-state value.

Comparison of the different plasma components transport can be the important tool for characterization of plasma turbulence conditions. In the case of neoclassical plasma, the different plasma ions should have different confinement times, in contrast to the conditions of high level of convective cells turbulence, where the transport should be the same for all plasma ions and electrons, because arising electric drift do not depend on the charge value and its sign. Such conditions were experimentally observed in experiments in T-4, were confinement times of hydrogen and argon were the same [4]. Later the same result was obtained in TFTR for hydrogen and iron confinement [8]. Recently similar experiment with tritium diffusion was carried out in JET [9], but no comparison with high *Z* impurities was reported. Thus the equal confinement of impurities and main plasma ions may evidence in

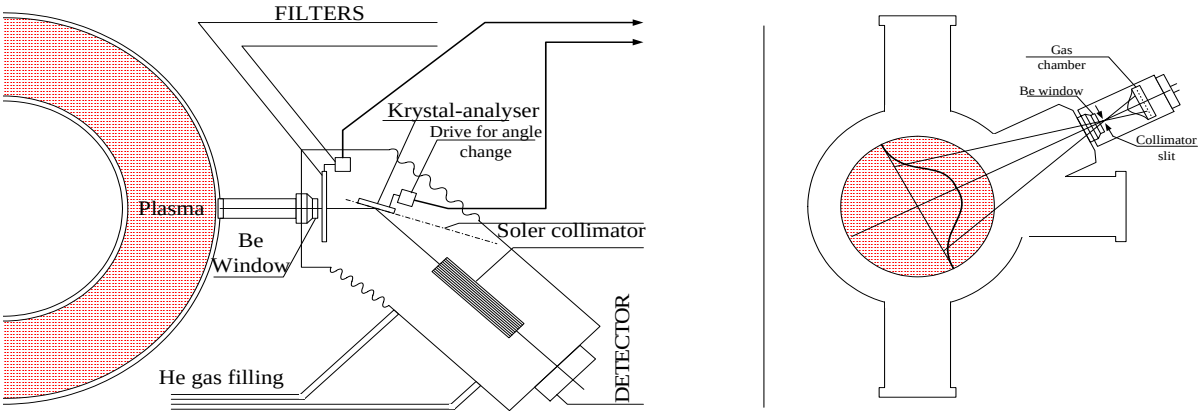

FIG. 2. Schematics of X-rays crystal monochromator with Soller collimator and proportional gas chamber. Left panel: Top view. Right panel: poloidal cross-section.

favor of the strong turbulence plasma condition. From other hand, the longer impurity confinement due to the neoclassical accumulation will show that anomalous turbulent transport is smaller then neoclassical one. At the same time, the development of the turbulence at the electron Larmour scale, or magnetic fluctuations could result in the additional losses of the electrons and their lower confinement with respect to ions. The measurements of the plasma potential in T-10 with HIBP [10] showed that in OH and, even in ECRH discharges, core plasma potential is negative, which evidences that ion diffusivity is higher, then electrons. In this case, the plasma diffusion should be determined by the electron component. Thus, the comparison of the different plasma species confinement may be informative about turbulence types and its level. Simultaneous investigations of the plasma transport and the turbulence characteristics may provide the experimental data, which will help to understand the physical mechanism of anomalous transport.

The confinement of high *Z* ions was studied using KCl, Ti pellets and fast argon gas injections. The impurities were added by the pneumatic injector. Their confinement was analyzed by means of X-ray crystal monochromator RM-2 [11]. The scheme of RM-2 is shown in Fig.2. It uses the pyrographite crystal as the spectral analyzer. The incident angle is determined by the Soller collimator. The space resolution across the plasma cross-section is obtained by the slit, mounted at the crystal. It was able to record the brightness of the He or H-like argon, potassium or titanium lines along the 48 chords simultaneously with the time resolution of 10 μs. The emission of each line was observed in a series of the reproducible discharges. The dynamic variation of He and H-like impurity ions after injection was modeled with the special code, solving ionization, recombination and diffusion of all impurity ion [12]. The simulations ensure that even at temperatures 2.5 keV the time behavior of the He and H-like impurity lines were similar, because the ionization equilibrium time was less, then the diffusion one. Main plasma confinement was investigated, using short D_2 gas puff. The dynamic evolution of the local density was done with the Abel inversion of the 16 channels mm-wave and infrared laser interferometer. The energy confinement time was estimated from the total heating power and total energy in plasma. Turbulence characteristics were measured by correlation reflectometer (CR) [1], from LMFS (at the angle 60 degrees to the equatorial plane of the plasma torus) and later from the HMFS launch.

The confinement times were determined during the last phase of the injection, when plasma parameters already return to the stationary values and the perturbations are negligible. It should be noted that during 10 – 15 ms after injection plasma parameters and the turbulence were significantly perturbed and the features of so-called non-local diffusion were seen. But this phenomenon is out of scope of the paper. The dependence of the impurity confinement on plasma density in OH regimes, has been investigated in T-10 previously [5]. These results are

shown in Fig. 3 together with the new impurity and energy confinement data. The discharge conditions were I_p=200 kA and B_T=2.3 T. It is clearly seen that impurity and energy confinement are equal each other. Moreover, both data reveal the well known feature. The confinement rises with density up to 0.5 of the Greenwald limit and after that saturate. Recent results of impurity confinement agree well with the old one. The impurity confinement is equal to the energy with the exception of high densities region, where a great scatter of the data from 40 to 240 ms was observed. In order not to increase the scale, the ordinate axis was broken and the scale of the top was changed in Fig. 3. The analysis of discharges with high impurity confinement reveals the fact that accumulation occurs in dirty plasma, where sawteeth activity is suppressed and neoclassical impurity accumulation takes place mainly in the plasma centre. This proves well known phenomenon that plasma transport near the axis is close to neoclassical in OH discharges. At the same time in the clean conditions, sawtooth activity was sustained and the lowest confinement of 40 ms. was observed. It reveals the fact that the transport in the gradient zone of the discharge was highly anomalous. The coincidence of the impurity and energy confinement times is the evidence of the fact that plasma transport in OH is dominated by the turbulent convective cells with dimensions larger then the ion Larmour radius. Such cell could transport all plasma species with the same rate. The typical radial correlation length of the density fluctuations lies in the range 0.5-1.5 cm. [1]. In order to compare T-10 results with the scalings, from the other tokamak, the Alcator [13] and JET/TORE SUPRA [14] scalings for impurity confinement times are presented. Clearly seen, that JET/TORE SUPRA scaling very near to the experimental points, while Alcator gives twice higher values and does not depend on density. In addition ITER scaling for energy confinement time in OH discharges [15] is plotted. It gives slightly higher values then T-10 experiment.

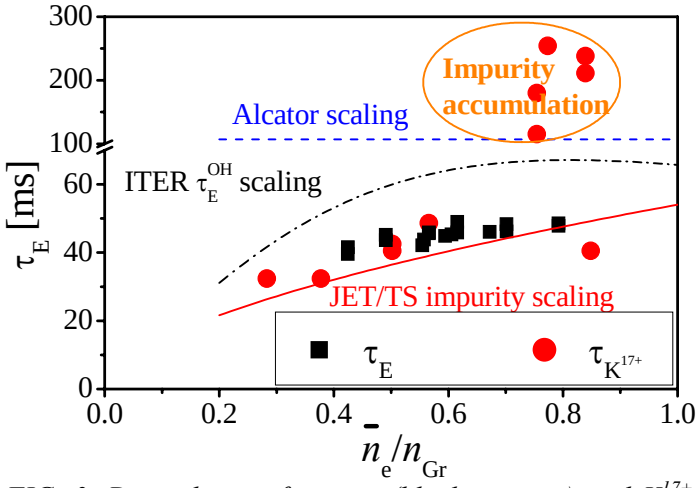

FIG. 3. Dependence of energy (black squares) and K^{17+} (red circles) confinement times from normalized electron density in Ohmic discharge with I_p = 200 kA. Greenwald density was $n_{Gr}=7.1\cdot10^{19}$ m^{-3}. Alcator (blue), ITER Ohmic (black) and JET/TORE SUPRA scalings are shown.

The dependence of different plasma species confinement versus average density in ECR heated discharges is plotted in Fig.4. The discharge conditions were I_p=200 kA and B_T = 2.3-2.5 T and central ECRH power 0.8-1 MW. The points of the Ti and electron density confinement are plotted together with the energy confinement in the previous [16] and new experiments. One can see that although the values are greatly reduced with respect to OH case, the qualitative density dependence is similar and the electron density and impurity confinements are close. The relation between impurity and electron confinement with energy confinement is illustrated with additional data in Fig.5. The discharge conditions were I_p=250 kA and B_T = 2.4 T and central ECRH power 1 MW. The linear rise of the confinement of all species is clearly seen at low densities. Although the values of impurity and electron density confinement are close each other, their values seems 20-30% higher, then the energy. The coincidence of the impurity and electron density confinement may point out that all ions and electrons have the same diffusivity. The lower energy confinement (determined mainly by electrons) with respect to ions may be regarded as the appearance of the additional loss channel in electron component. This may be the destabilization of the drift waves with the

electron Larmour scale or other short wave turbulence. For comparison in Fig. 4 and 5 the impurity JET/TORE SUPRA [14] and ITER L-mode energy confinement [15] scalings also plotted. Both scalings give similar values and reasonably coincides with T-10 experimental points. This coincidence should be specially noted because the ITER and JET/TORE SUPRA scalings were obtained mainly from the discharges with ion temperature comparable or much higher then electron one. In contrast, in T-10 with ECR heating the temperature ratio is reversed. Thus, even in the conditions of $T_e > T_i$, the ions confinement is still close to electron one. It means that even at higher electron temperature there is no any substantial additional losses with the electron heat conduction.

The dependence of the Ti and energy confinements on the power in OH and the central ECRH is shown in Fig.6. The discharge conditions were I_p=200 kA, B_T=2.3 T and average density n_e about 3×10^{19} m^{-3}. The central ECRH power varied from 0.4 to 1.4 MW. The dashed line presents the ITER "L" mode scaling [14]. It is seen that the energy confinement decreases with power in good agreement with the scaling. The Ti confinement also degraded, but to less extend. This fact is in good correlation with the impurity JET/TORE SUPRA [14] scaling, because it depends on heating power as $P^{-0.56}$, while energy confinement as $P^{-0.73}$. One can see that Ti confinement at highest power about 20-30 % higher, then energy. This supports the data of the Fig.5 and may point out additional electron losses at high ECRH power.

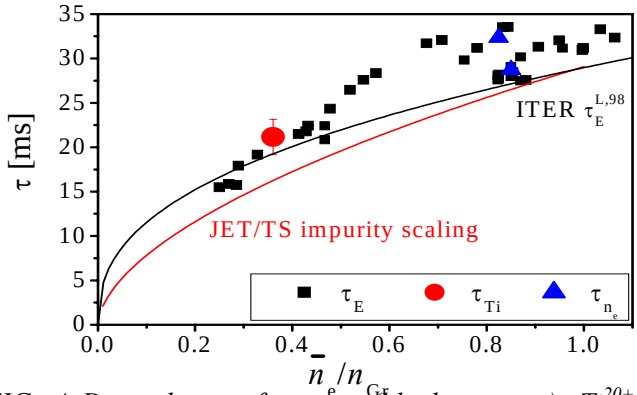

FIG. 4 Dependence of energy (black squares), Ti^{20+} (red circles) and electron density (blue triangles) confinement times from normalized electron density in ECRH discharge with I_p = 200 kA, P_{ECRH} = 0.8 MW. Greenwald density was $n_{Gr}=7.1\cdot10^{19}$ m^{-3}. ITER L-mode (black) and JET/TORE SUPRA scalings are shown.

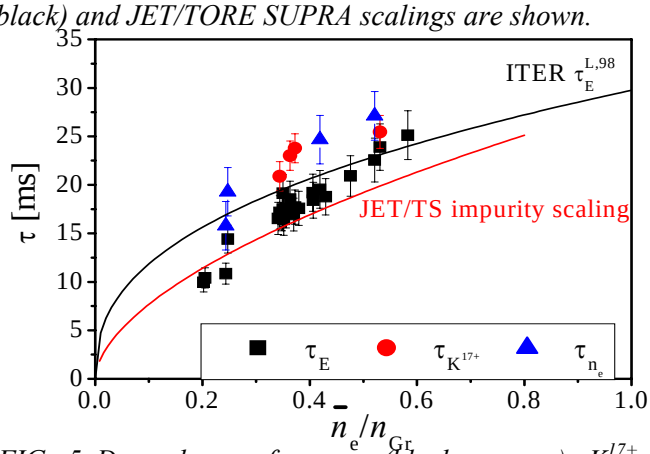

FIG. 5 Dependence of energy (black squares), K^{17+} (red circles) and electron density (blue triangles) confinement times from normalized electron density in ECRH discharge with I_p = 250 kA, P_{ECRH} = 1.0 MW. Greenwald density was $n_{Gr}=8.8\cdot10^{19}$ m^{-3}. ITER L-mode (black) and JET/TORE SUPRA scalings are shown.

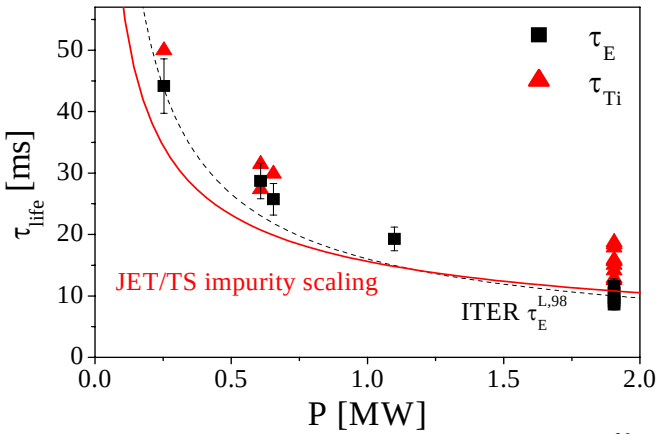

FIG. 6. Depencence of energy (black squares) and Ti^{20+} (red triangles) confinement times from total power in discharge with I_p = 200 kA. ITER L-mode (black) and JET/TORE SUPRA scalings are shown.

3. Turbulence characteristics at High Magnetic Field Side.

Reflectometry measurements of the density fluctuations characteristics were made with the T-10 correlation reflectometry with LMFS antennas (at the angle 60

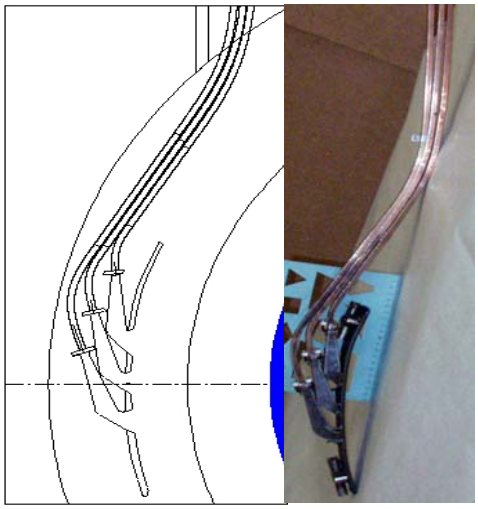

FIG. 7. Reflectometer antenna array at the HMFS on T-10 tokamak. Left panel: CAD drawing; right panel: antenna before the installation.

degrees to the equatorial plane of the torus) [1]. The measurements were made at a half of minor radius and show that long wavelength turbulence replaced by shorter one, while density increases up to half of the Greenwald density. The typical poloidal wavelength of turbulence decreases from 4 to 1.5 cm. This transition of the turbulence wavelength was completed at the half of the Greenwald density. So the turbulence wavelength became constant at higher densities. The confinement of the all plasma particles and energy are equal in OH plasma and exhibit the linear rise at low densities with the following saturation. These results strongly support that in OH plasma transport is dominated by the electrostatic drift convection, caused possibly by ITG and DTEM or other type instabilities. The other important factor is the strong decrease of the T_e/T_i ratio with the increase of density. This can also cause the rise of confinement.

The new experimental data, which characterize the poloidal turbulence structure, became possible using new HMFS antenna array installed in T-10 tokamak recently, which uses low frequency extraordinary wave. HMFS antenna system consists of three antenna horns with mouth size 25×27.5 mm, placed side-by-side in poloidal direction (Fig. 7). The electro-magnetic modeling shows that antenna forms rather narrow microwave beam that is propagating perpendicular to the antenna mouth. The mock-up measurements at frequency 30 GHz shows that beam width was about 30 degrees that is in good correlation with calculations results. Side lobe magnitude is rather small and cannot interfere with measurement results. The variations of the electric field vector of the reflected wave have been analysed in the frequency range 0–400 kHz by means of simultaneous recording of several channels using ADCs with a sampling rate of 0.8 MHz. The amplitude (A) and the phase (φ) fluctuations of the electric field vector were decomposed in imaginary ($U_1 = A\sin(\varphi)$) and real ($U_2 = A\cos(\varphi)$) parts. Signals were processed in the complex form. Routine T-10 correlation reflectometry system [1] was used to compare turbulence characteristics from Low Magnetic Field Side (LMFS) (placed at the poloidal angle 60 degrees to equatorial plane) with those for HMFS.

First experiments show that the turbulence level at HMFS is small in plasma core region. The results of correlation analysis of reflectometer signals reflected from HMFS in Ohmic discharge shown in Fig. 8. As one can see turbulence spectra contains the same components as at the LMFS. Broad Band (BB) and Low Frequency (LF) fluctuations dominate in spectra while Quasi Coherent (QC) oscillations is smaller that at the LMFS in accordance with gyrokinetic simulation results [17]. The fluctuations in frequency range 15-30 kHz that is often interpreted as Geodesic Acoustic Modes was not observed in equatorial plane at

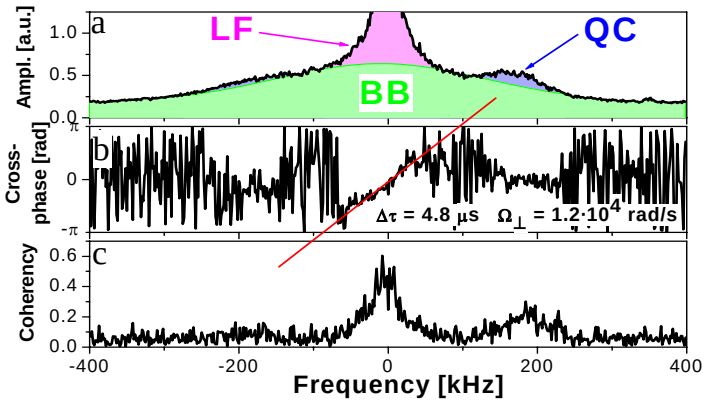

FIG. 8. Fourier spectra of spectra (a) , poloidal cross-phase (b) and coherency (c) at HMFS. Discharge parameters was $B_T = 2.4$ T, $\langle n_e \rangle = 2.9\times10^{19} m^{-3}$, $\rho \sim 0.35$.

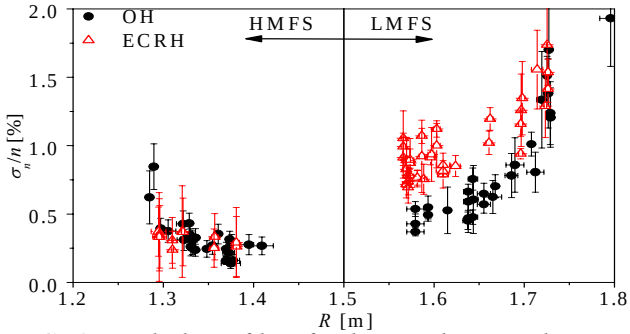

FIG. 9. Radial profile of relative electron density perturbations amplitude in Ohmic and ECRH discharges with $I_p = 300$ kA, $B_T = 2.45$ T, $\langle n_e \rangle = 3\times10^{19}$ m^{-3}, $P_{ECRH} = 1.5$ MW.

HMFS yet. This fact could be considered as additional conformation of the hypothesis that this oscillation is GAM. Poloidal coherency of fluctuations is high enough to provide the velocity measurements. Radial profile of the relative amplitude of density fluctuations was measured in series of reproducible discharges with $I_p = 300$ kA, $B_T = 2.45$ T, $\langle n_e \rangle = 3\times10^{19}$ m^{-3}, by varying reflectometer frequency (Fig. 9). Total power of central heating at second harmonic of electron cyclotron resonance (ECRH) was about 1.5 MW. Algorithm proposed in [18] was used to reconstruct the amplitude of density fluctuations from reflectometer data.

One can see that density fluctuation profile at HMFS shows the same properties as at LMFS: fluctuations amplitude is constant in plasma core and significantly increase at plasma periphery. However, the amplitude of fluctuations has strong poloidal asymmetry. In Ohmic discharges density fluctuations amplitude in gradient region was 0.25 % at HMFS in comparison with 0.5 % at LMFS at the top. This asymmetry increased during ECRH because the turbulence level increased at LMFS up to 1 % and remains the same at HMFS. Such behavior justifies the simulation results and theoretical opinion that main origin of instability in tokamak is unfavorable curvature of magnetic field at the external side of plasma column.

Although fluctuations amplitude not changed at HMFS, certain variations observed in signal spectra (Fig. 10). All spectra were normalized in the way, based on [18], to represent the spectra of local density fluctuations. In Ohmic phase of discharge, the spectrum at HMFS has a QC component at frequencies about 150 kHz. QC oscillations completely disappear during ECRH at HMFS while at LMFS one can see strong QC modes. This fact could be explained in following way: fluctuations arise due to excitation of instabilities at LMFS. Further evolution of the system leads to formation of radially elongated structures (“fingers”) that were achieved both in theory [19] and in 3D simulations [17]. Then density perturbations propagate along the magnetic field line and reach HMFS. Amplitude and contrast of QC oscillations decrease during ECRH and it leads to disappearing of QC at HMFS. This hypothesis is rather rough and further investigation is required both from experiment and from theory to reveal this question.

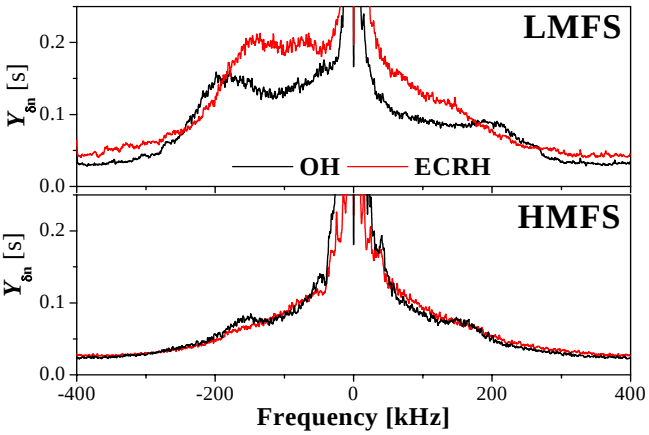

FIG. 10. Fourier spectra of density perturbations at LMFS (top panel) and LMFS (bottom panel). Discharge parameter the same as in FIG. 9.

4. Conclusions

The observed results it is possible to summarize as follows:

1. The equal values and similar density dependences of impurity, electron density and energy confinement times in OH discharges may suggest that all transport processes are determined by the same physical processes, like convective cells. Nevertheless, it should be noted that the energy confinement is measured in steady

state condition, while impurity and electron density confinement uses dynamic measurements. So one should be careful in comparing these times.

2. T-10 results with ECR heating show that even in the conditions of $T_e > T_i$ the ion confinement still close to energy one, which is mainly determined by electron heat conductivity. This is also the case at the low densities, where T_e/T_i ratio may reach a factor of 10. It means that even in discharges with dominant electron temperature there is no any substantial additional electron heat conduction losses with respect to ions.
3. The energy confinement times decrease with heating power as $P^{-0.73}$ in accordance with ITER "L"-mode scaling.
4. Slightly lower decrease rate of the ion confinement may be the evidence of additional losses of electrons with the short-wave turbulence such as ETG or magnetic fluctuations. The higher electron losses in ECRH plasma is supported by increase of plasma potential, measured with HIBP.
5. Transition of the turbulence type from long wave to the short wave turbulence may be the reason of the confinement rise at low densities
6. Fluctuations amplitude in Ohmic discharges lower in a factor 2-3 at HFS in comparison with LFS and does not increase during ECRH in contrary to LFS. Thus the asymmetry rises with the increase of the input power. This implies the important role of the toroidal effects in turbulence increments.
7. All spectral components are seen at HMFS in turbulence spectra except the "20 kHz" mode (GAM), but their relative values are different.

This work is supported Nuclear Science and technology Department of Minatom RF, Scientific School 1608.2003.2, RFBR (Grant 04-02-17567, 02-02-17727), NWO 047.016.015 and INTAS (Gr. 2001 - 2056)

References

[1] Vershkov V.A. et al, Nuclear Fusion, **45** (2005) S203.
[2] Vershkov V.A., Mirnov S.V., Nuclear Fusion 14 (1974) p. 383.
[3] V.A. Abramov, et al, 8th EPS Conf. Cont. Fus. Plasma Phys., Prague (1977) V. 1, p. 30.
[4] Buzankin V.V. *et al*, Plasma Phys. Cont. Fus. Res., 1978, IAEA, Vienna (1979) **1**, 287
[5] A.A. Bagdasarov, et al, Plasma Physics and Controlled Fusion Research, 1984, IAEA, Vienna (1985) Vol. 1, p 181
[6] A.A. Bagdasarov, et al, Proc. of 12th EPS Conf. Cont. Fus. Plasma Phys., 1985, Budapesht, Hungary, V. 1, p. 207.
[7] V.A. Vershkov, et al, Fizika Plazmi, 1989, V 15, #. 4, p. 387 (in Russian).
[8] K.W. Hill, et al, Proc. of 11th Int. Conf. on Plasma Physics and Contr. Nucl. Fusion Research, 1986, Kyoto, Japan, IAEA, Vienna (1987) V. 1, p. 207
[9] K.D. Zastrov, et al, Plasma Physics and Controlled Fusion, V 46, # 12B (2004) p B255.
[10] Melnikov A.V. *et al*, Proc. 32nd EPS Conf. Plasma Phys. 2005 P4-052
[11] Vershkov V.A. *et al* "Pribory and Technika Experimenta", **6**, 1987, 171 (in Russian).
[12] Yu. N. Dnestrovskii, V. F.Strijov, Preprint "Kurchatov Institute", 1983, KIAE – 3779/6
[13] E.S. Marmar,et al, Nuclear Fusion, V 22 (1982) p 1567.
[14] M. Mattioli, et al, Nuclear Fusion, V 35 (1995) p 1115.
[15] ITER Physics Basis, Nuclear Fusion, **39** (1999) 2137
[16] Yu. V. Esipchuk, *et al*, Plasma Phys. and Cont. Fus., **45**, (2003) 793.
[17] Lin Z. *et al* 1998 Science **281** 1835
[18] D.A. Shelukhin *et al*, 2006, Plasma Physics Reports, **32** (9) 707
[19] Romanelli F., Zonca F. 1993 Phys. Fluids B **5** (11) 4081